# APPARATUS ARCHITECTURE OF THE CONODONT *NICORAELLA KOCKELI* (GONDOLELLOIDEA, PRIONIODININA) CONSTRAINS FUNCTIONAL INTERPRETATIONS

*by* JINYUAN HUANG[1,2,3,4,*] (iD), CARLOS MARTÍNEZ-PÉREZ[2,5], SHIXUE HU[1], QIYUE ZHANG[1], KEXIN ZHANG[3], CHANGYONG ZHOU[1], WEN WEN[1], TAO XIE[1], MICHAEL J. BENTON[5] (iD), ZHONG-QIANG CHEN[6], MAO LUO[7] *and* PHILIP C. J. DONOGHUE[5,*] (iD)

[1]Chengdu Center of China Geological Survey, Chengdu 610081, China; hjinyuan@cgs.cn
[2]Cavanilles Institute of Biodiversity & Evolutionary Biology, University of Valencia, 46980 Valencia; Spain
[3]Institute of Geological Survey, China University of Geosciences (Wuhan) Wuhan 430074, China
[4]State Key Laboratory of Palaeobiology & Stratigraphy (Nanjing Institute of Geology & Palaeontology, CAS), Nanjing 210008, China
[5]School of Earth Sciences, University of Bristol, Life Sciences Building, Tyndall Avenue, Bristol, BS8 1TQ, UK; phil.donoghue@bristol.ac.uk
[6]State Key Laboratory of Biogeology & Environmental Geology, China University of Geosciences, Wuhan 430074, China
[7]State Key Laboratory of Palaeobiology & Stratigraphy, Nanjing Institute of Geology & Palaeontology & Center for Excellence in Life & Palaeoenvironment, Chinese Academy of Sciences, 39 East Beijing Road, Nanjing 210008, China
*Corresponding authors

**Abstract:** We reconstruct the apparatus architecture of the gondollelid conodont *Nicoraella kockeli* based on fused clusters from the early Middle Triassic (middle Anisian, Pelsonian) of Luoping County, east Yunnan Province, south-west China. This material was characterized non-invasively using synchrotron x-ray tomographic microscopy and the ensuing data analysed using computed tomography, allowing us to infer the composition, homologies and architectural arrangement of elements within the apparatus. Much of the original three-dimensional architecture of the apparatus is preserved and our apparatus reconstruction is the best characterized of any taxon within the superfamily Gondolelloidea. This allows us to test architectural models for gondolelloids and prioniodinins, more generally, as well as the functional interpretations based upon them. In particular, we reject a recent functional interpretation of the conodont feeding apparatus which was based on a biomechanically-optimized inference of apparatus architecture in a close gondolelloid relative of *Nicoraella*. Nevertheless, our architectural model provides a foundation for future functional interpretations of gondolelloids and prioniodinins, more generally.

**Key words:** structure, function, conodont apparatus, Middle Triassic, SW China.

CONODONTS are among the most diverse clades of jawless vertebrates and they are abundant components of Palaeozoic and early Mesozoic marine ecosystems. However, their role within those ecosystems has been unclear because of controversy surrounding the functional interpretation of their feeding apparatus, which comprised the eponymous tooth-like elements that dominate the conodont fossil record. Conodont functional morphology has a long history of poorly constrained speculation and, indeed, for much of this time, debates over the affinity of conodonts and the function of their elements were inextricably linked. The identification of conodont element-like structures in diverse metazoans, plants and even fungi inspired both functional interpretations of the elements and phylogenetic interpretations of the host organism (Aldridge 1987). Separation of debates over affinity and function awaited the discovery of soft tissue remains of conodonts (Briggs & Fortey 1982), but subsequent research demonstrated that it had always been possible to independently constrain, develop and test hypotheses of element function based on articulated skeletal assemblages that preserve the collapsed remains of the feeding apparatus of a single conodont individual (Aldridge *et al.* 1987, 1995, 2013; Purnell & Donoghue 1997, 1998, 1999).

First discovered in the early 1930s (Schmidt 1934; Scott 1934), 'natural assemblages' preserve elements of different morphology in a limited series of different relative arrangements, interpreted originally to reflect post-mortem muscle

and ligament contortion and contraction (Collinson *et al.* 1972). These arrangements were subsequently shown to reflect different collapse orientations of the same original three-dimensional construction, that can be 'solved' by a three dimensional physical model which, when viewed from different perspectives, simulates the relative arrangement of elements in natural assemblages and, thus, the original orientation of collapse (Aldridge *et al.* 1987). Such models have been built for disparate conodont clades, demonstrating collectively that the natural assemblages of most 'complex conodonts' can be explained by the model derived from *Idiognathodus* (Purnell & Donoghue 1997). More recently, a different architectural arrangement was inferred for the Early Triassic *Novispathodus*, interpreted to reflect different element positions within a functional cycle (Goudemand *et al.* 2011). This architecture was based in part on a heuristic biomechanical analysis of the optimal functional and positional arrangement of elements, inspired by partial fused natural assemblages of *Novispathodus* and complete but compressed bedding plane natural assemblages of *Neogondolella* (Goudemand *et al.* 2011). Overall, their analysis suggests that different conodont taxa exhibit different element architectures.

Here, we reconstruct the apparatus of *Nicoraella kockeli* based on a collection of fused natural assemblages from the early Middle Triassic (middle Anisian, Pelsonian) of Luoping County, east Yunnan Province of south-west China (Huang *et al.* 2018, in press). *Nicoraella kockeli* is a close relative of *Novispathodus* and *Neogondolella*, allowing us to test the architectural and functional models proposed by Goudemand *et al.* (2011). We find that the functional model presented by those authors contradicts primary anatomical evidence in the fossils from which it was derived. As such, both should be rejected. Finally, we present an accurate reconstruction of the feeding apparatus of *Nicoraella* and consider its implications of apparatus architecture for hypotheses of function.

## MATERIAL AND METHOD

Our study is based on four articulated clusters from the Luoping Konservat-Lagerstätte in Luoping County, Yunnan Province, south-western China. The Luoping Biota encompasses a diverse assemblage of microfossils (conodonts, foraminifers, ostracods, etc.) as well as articulated macrofossils including planktonic marine reptiles, fishes, benthic echinoderms (crinoids, sea urchins, sea cucumbers and sea stars), bivalves, gastropods, belemnoids, ammonoids, brachiopods, arthropods (decapods, isopods, limulids and cycloids), trace fossils and a few terrestrial plants and millipedes (Hu *et al.* 2011).

The fossiliferous sediments occur within the Guanling Formation (Member II), which is composed, in succession,

of a dark micritic nodular limestone, followed by a micrite bearing chert nodules or siliceous bands, followed by a micrite with dolomite (Zhang *et al.* 2009). The clusters come from several limestone layers in the lower thin-bedded unit of Dawazi Section, which consists mainly of thin laminar micritic limestone intercalated with prominent cherty nodules. It is dated to the Pelsonian substage of the Anisian (Middle Triassic), based on the presence of the conodont *Nicoraella kockeli* (Huang *et al.* 2009, 2011).

The element clusters attributable to *Nicoraella kockeli* were obtained through acid digestion (6% acetic acid) of the limestone samples. The clusters are preserved in only a partially compressed state, maintaining considerable three dimensionality in the arrangement of the elements which are bound together by diagenetic calcium phosphate. All specimens are deposited at the Chengdu Center of China Geological Survey (CDCGS). The most complete clusters were characterized using synchrotron-radiation x-ray tomography (SRXTM), using the X02DA TOMCAT beamline at the Swiss Light Source, Paul Scherrer Institute (Villigen, Switzerland), a nondestructive technique that permitted us to establish the morphology and relative arrangement of the elements comprising the clusters using computed tomography (Donoghue *et al.* 2006). The samples were scanned using a 20× objective, at 10–17 KeV with an exposure time between 180 and 350 ms, acquiring 1501 projections equiangularly over 180°. Projections were post-processed and rearranged into flat- and dark-field-corrected sinograms, and reconstruction was performed on a 60-core Linux PC farm using a Fourier transform routine and a regridding procedure (Marone *et al.* 2010). The resulting volume has isotropic voxel dimensions of 0.325 μm. These data are available in Huang *et al.* (2018). Slice data were analysed and manipulated using the computed tomography software Avizo 8 (https://fei.com). Finally, renderings were manipulated using the software Geomagic Studio v. 12 (Geomagic, Rock Hill, SC, USA) to reconstruct digitally the apparatus structure and simulate the different collapse orientations represented by the fused natural assemblages. Virtual models of the isolated elements and the reconstructed apparatus are available in Huang *et al.* (2019*a*).

Previously, researchers have inferred apparatus architecture through physical modelling, arriving at a single solution that, when viewed from different orientations, simulates the collapse orientation represented in the natural assemblages (Aldridge *et al.* 1987, 1995, 2013; Purnell & Donoghue 1997, 1998). We followed an analogous approach, building a digital three-dimensional model (Fig. 1) based on the virtual elements segmented using computed tomography from the tomographic characterizations of the cluster preserving the largest number of elements (pm028-18-wy1-C1; Fig. 2A–C). Following the physical modelling approach, we adjusted the relative arrangement
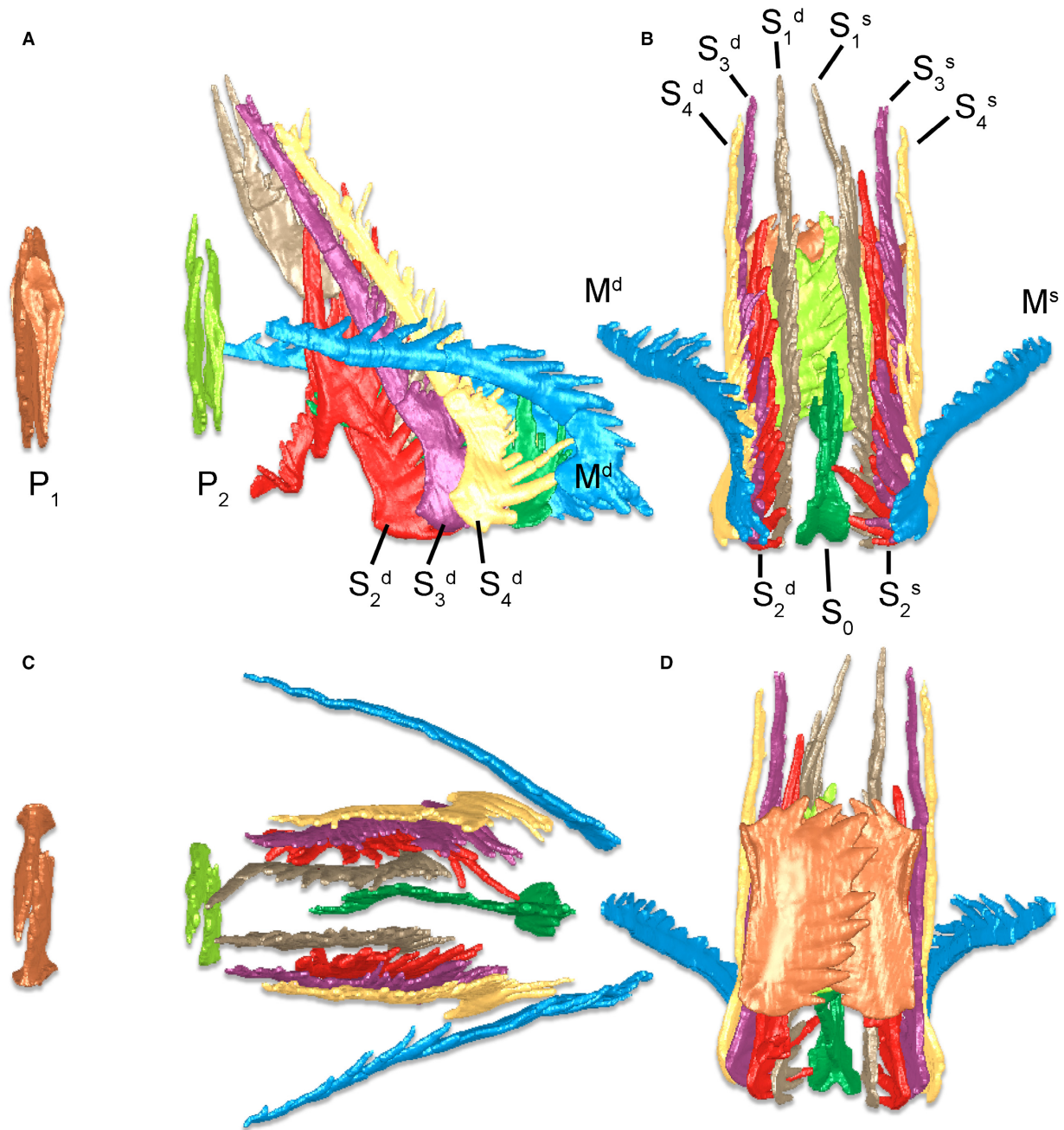
**FIG. 1.** *Nicoraella kockeli* conodont apparatus architecture and notation reconstructed from the fused clusters natural assemblages described here, using virtual models of the elements from cluster pm028-18-wy1-C1 (Fig. 2A–C). A, lateral; B, rostral; C dorsal; and D, caudal views of the apparatus.

of the elements until we arrived at a single model in which the core aspects of element arrangement could be replicated by viewing the virtual model from different orientation, simulating the direction of collapse. Though we had access to many tens of fused natural assemblages (Huang *et al.* 2019*b*), only a small number of these were composed of enough of the apparatus to prove useful in reconstructing the original apparatus architecture. Furthermore, these

assemblages preserve a limited number of collapse orientations and, therefore, perspectives on the apparatus; by their nature, complete fused clusters are limited to orientations in which all of the elements overlap one another, or they would not be fused together (Huang *et al.* 2019*b*). However, a number of the clusters exhibit limited collapse, preserving aspects of the original spacing and relative arrangement of the elements within the apparatus, not
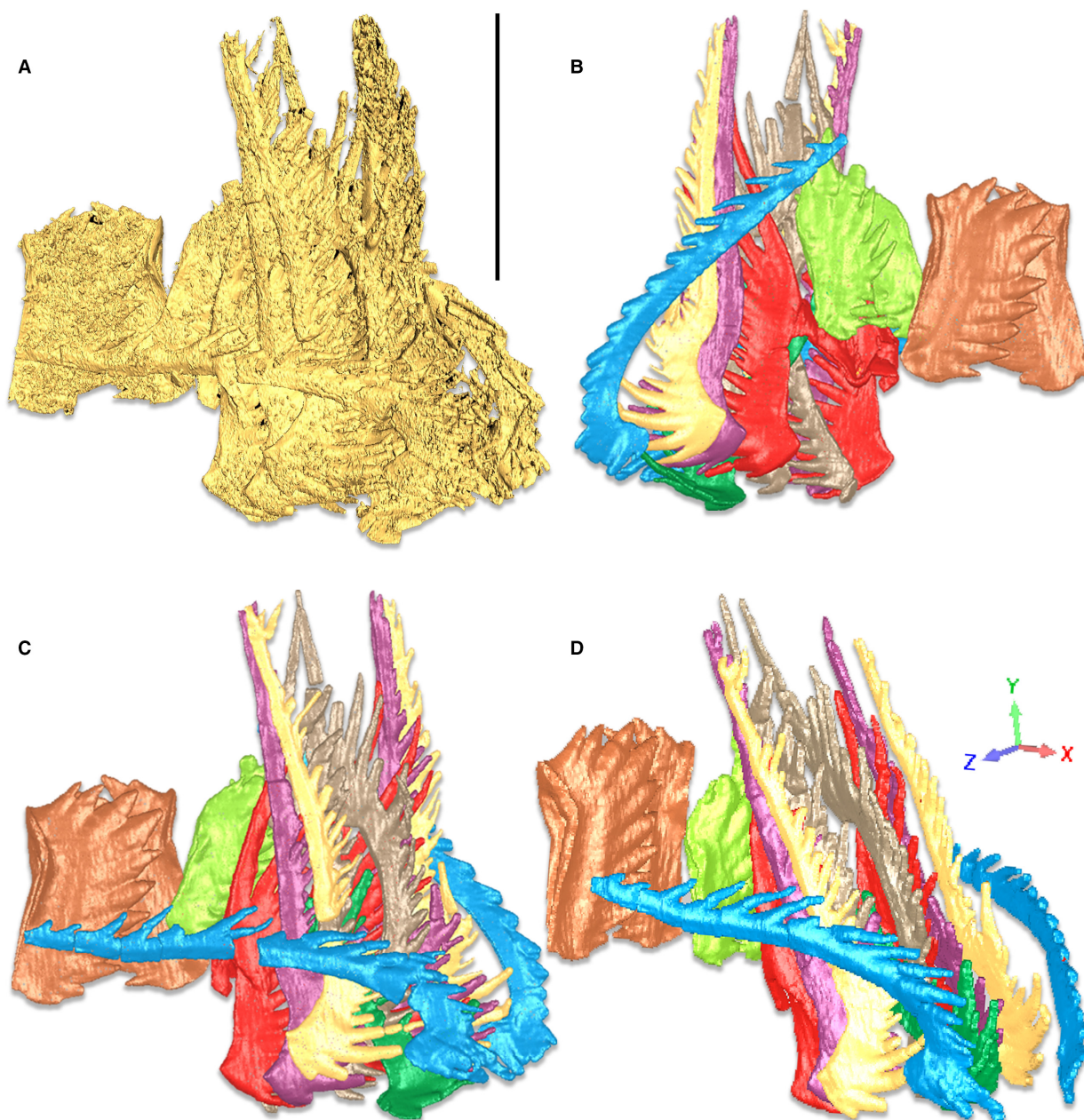
**FIG. 2.** Isosurface and segmented model of the *Nicoraella kockeli* cluster pm028-18-wy1-C1 derived from SRXTM data containing the 15 elements of the apparatus. A, isosurface model of the cluster. B–C, segmented model in left and right views. D, virtual model of the reconstructed apparatus simulating the direction of collapse. Scale bar represents 400 μm.

usually seen in fused cluster natural assemblages (Nicoll 1982, 1985; Nicoll & Rexroad 1987; Mastandrea *et al.* 1997; Schülke 1997; Goudemand *et al.* 2011). Nevertheless, we reconstructed the apparatus by first arranging the elements of *Nicoraella kockeli* according to the architecture of *Polygnathoides* (Purnell & Donoghue 1998) before adjusting the relative position and orientation of the elements to simulate the collapse orientations of the fused cluster natural assemblages of *N. kockeli*.

Following Purnell *et al.* (2000), we describe the orientation of elements and element processes with reference to their traditional within-element orientations ('anterior', 'posterior', etc., with reference to the cusp) and their natural biological orientations (rostral–caudal, dorsal–ventral, sinistral–dextral) with reference to the orientation of homologous elements in specimens of *Clydagnathus winsorensis* preserving soft tissue anatomy, from the Mississippian Granton Shrimp Bed of Granton, Edinburgh (Aldridge *et al.* 1993).
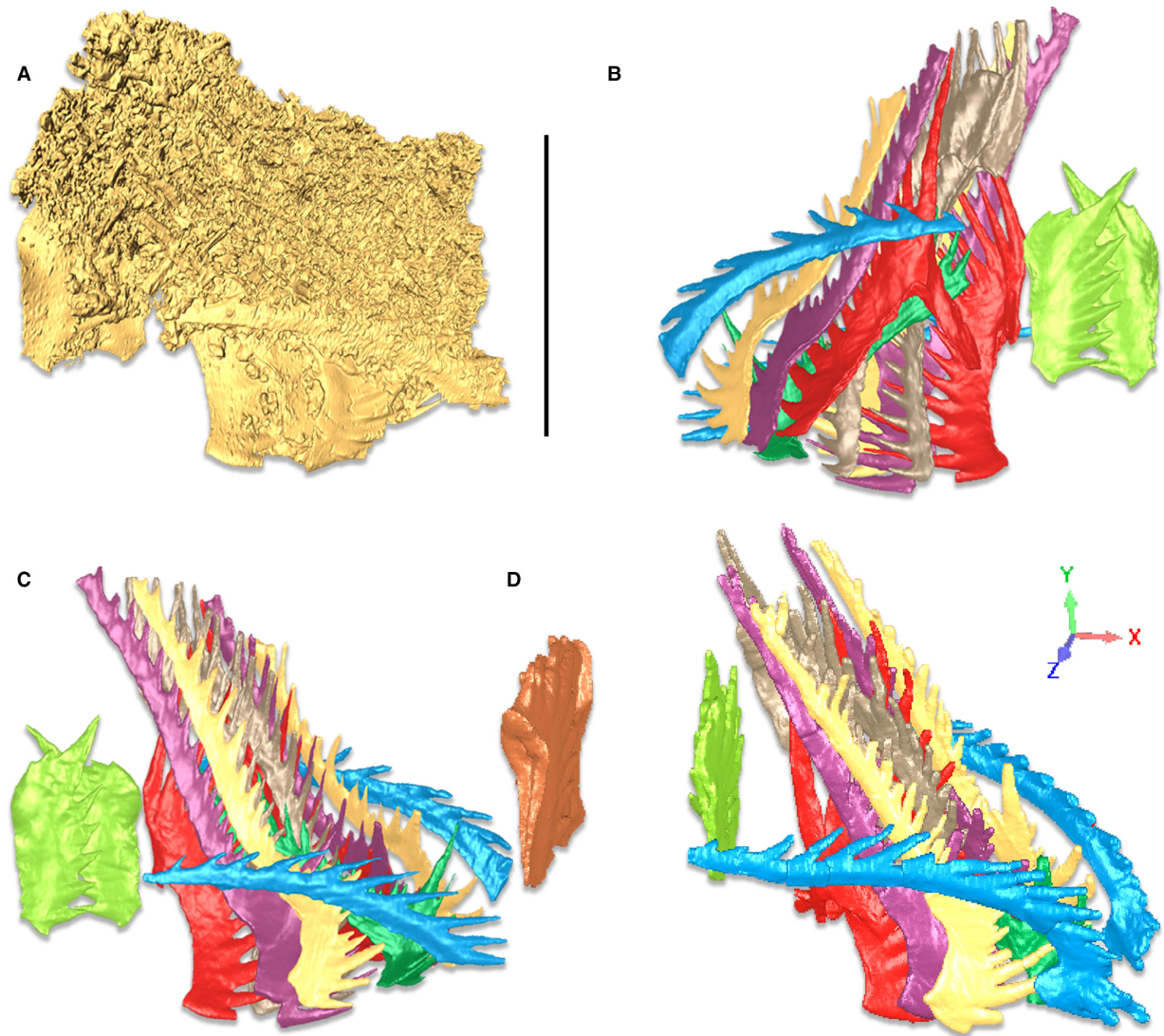
**FIG. 3.** Isosurface and segmented model of the *Nicoraella kockeli* cluster pm028-25-wy1-C1 derived from SRXTM data containing 13 elements of the apparatus. A, isosurface models of the cluster. B–C, segmented model in left and right views. D, virtual model of the reconstructed apparatus simulating the direction of collapse. Scale bar represents 400 µm.

## RESULTS

### Cluster composition

Four clusters were characterized using SXRTM. These differ in terms of the number of elements present, with one cluster composed of 15 elements (Fig. 2), another of 13 (Fig. 3), and two clusters composed of 11 elements each (Figs 4, 5). All four clusters are composed of 11 ramiform elements, including five symmetrical pairs of elements and a single, central, approximately symmetrical alate element. Two of the clusters possess an additional symmetrical pair of elements of pectiniform morphology, while the cluster composed of 15 elements has a second pair of pectiniform elements. The relative arrangement of the component elements differs between clusters, comparable to those described previously from natural assemblages (Purnell & Donoghue 1998) and we interpret them as reflecting different collapse orientations of the same original three-dimensional arrangement of elements (Briggs & Williams 1981; Aldridge *et al.* 1987). A detailed description of the fused cluster natural assemblages is provided by Huang *et al.* (2019*b*, in press).
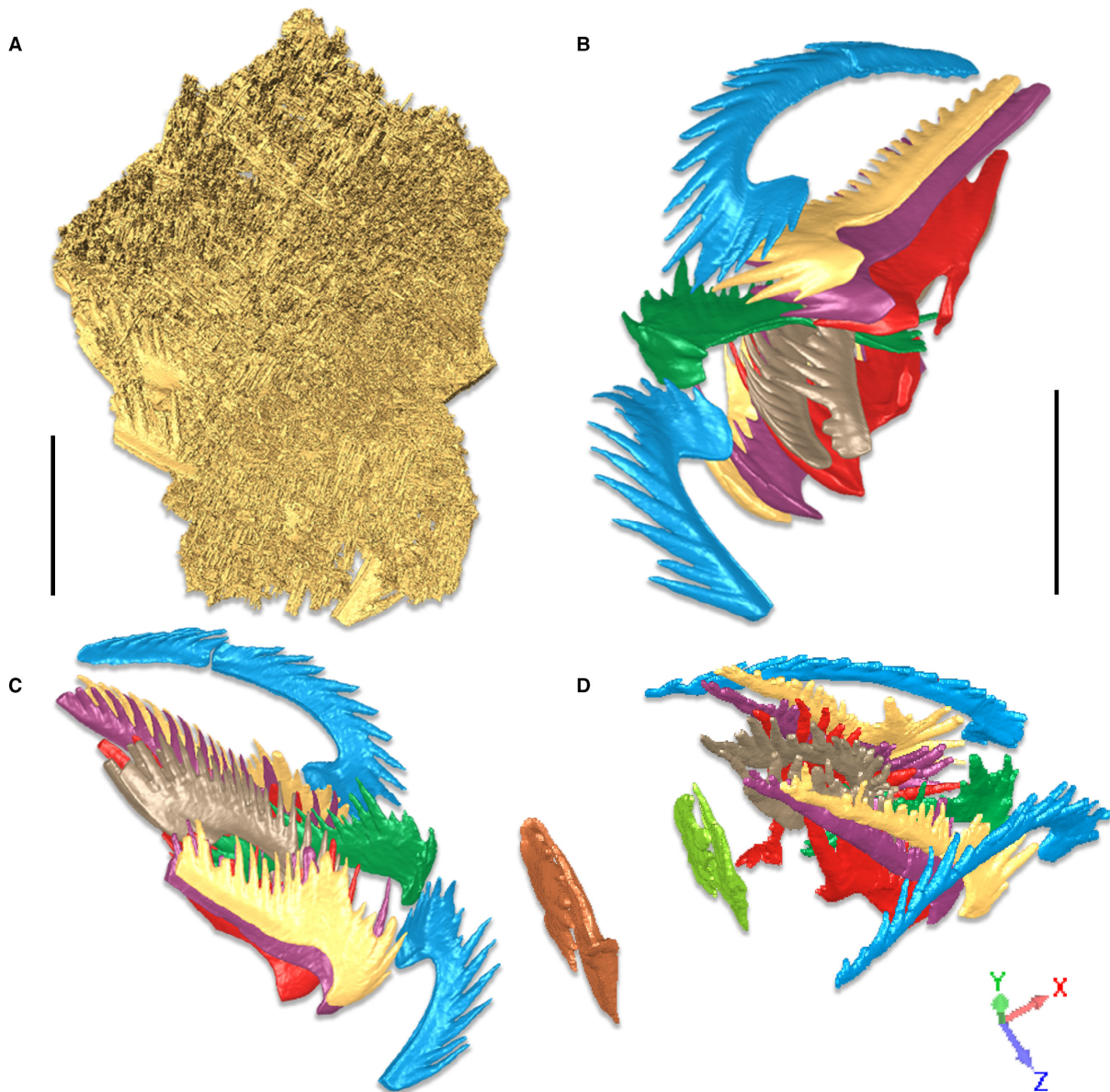
**FIG. 4.** Isosurface and segmented model of the *Nicoraella kockeli* cluster pm028-25-wy1-C2 derived from SRXTM data containing 11 elements of the apparatus. A, isosurface models of the cluster. B–C, segmented model in anterior oblique and left and lateral (slightly dorsal) views respectively. D, virtual model of the reconstructed apparatus simulating the direction of collapse. Scale bar represents 400 μm.

*Apparatus composition*

The inferred architectural model allows us to identify the homology of the component elements directly, based on their position within the apparatus (Fig. 1; Purnell *et al.* 2000), rather than on the basis of similarity in element morphology to taxa in which position homologies can be observed. Huang *et al.* (2019*b*, in press) established that the apparatus of *Nicoraella* is composed of 15 elements

(Fig. 1), including a pair of caudal pectiniform $P_1$ elements, a more rostral pair of pectiniform $P_2$ elements that overlap on the rostro-caudal axis with an array of ramiform elements. The ramiform array is composed of an alate axial $S_0$ with short lateral process and a long posterior process extending from the cusp. Abaxial, in order relative to the $S_0$, are symmetrical sinistral and dextral pairs of: (1) breviform dygyrate $S_1$ elements with a short antero-lateral process aligned ventrally, a
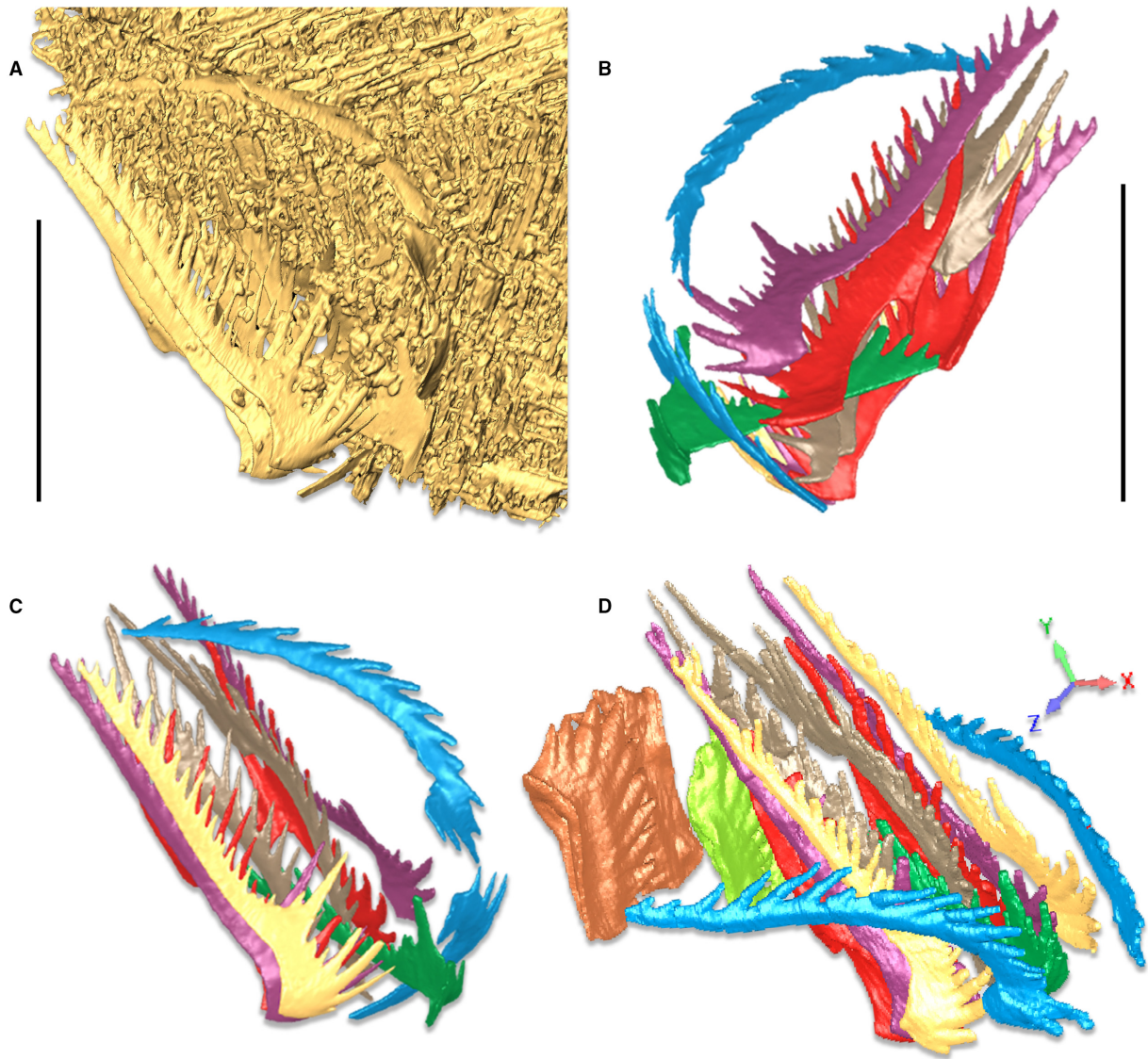
**FIG. 5.** Isosurface and segmented model of the *Nicoraella kockeli* cluster pm028-26-wy1-C1 derived from SRXTM data containing 11 elements of the apparatus. A, isosurface models of the cluster. B, segmented model in lateral (slightly ventral) view. C, segmented model in almost lateral view. D, virtual model of the reconstructed apparatus simulating the direction of collapse. Scale bar represents 400 μm.

caudally-directed cusp, and a long inner-lateral process that extends rostrally; (2) breviform digyrate $S_2$ elements with two antero-lateral processes, one robust abaxial process aligned rostrally and a less robust but equally long adaxial process that extends ventrally; (3–4) two morphologically similar bipennate elements with short anterior processes aligned rostrally with the adaxial antero–lateral processes of the $S_1$ and $S_2$ elements, and long posterior processes aligned dorso-caudally with the outer cusps of the $S_1$ and $S_2$ elements. The ramiform array is flanked abaxially by a pair of symmetrically arranged makellate M

elements that are oriented with their long, curved, inner-lateral process at about 60° to the bilateral axis, converging rostrally such that their cusps are directed horizontally and laterally, and their short outer-lateral process is oriented ventrally.

### Apparatus architecture

The elements within the apparatus of *Nicoraella* are arranged such that the $S_0$ occupies the most rostral

position (on the plane of bilateral symmetry) with its paired lateral processes and cusp positioned slightly rostrad relative to the rostral processes of the cusps of the $S_{1-4}$ elements that are positioned slightly caudad of one another. Otherwise, the S elements are all generally aligned in parallel with one another and the plane of bilateral symmetry, and at c. 55° relative to a horizontal plane. The M elements are oriented with their long axis c. 25° relative to the S elements and c. 45° to a horizontal plane, with the tips of their cusps in line with the rostral limit of the $S_0$. The long axes of the P elements are aligned approximately perpendicular to the horizontal plane; following Purnell et al. (2000), this 'anterior–posterior' axis of the P elements equates to the ventral–dorsal (respectively) axis of the organism. The P elements are positioned at mid-height (with respect to the S elements) on this dorso-ventral axis, occluded and with their sinistral elements positioned caudal to their dextral pair. The $P_2$ elements are positioned approximately halfway along the rostro-caudal axis: between the $P_1$ elements and the caudal 'posterior' tips of the $S_{3-4}$ elements. The $P_1$ elements are positioned caudad of the $P_2$ and $S_{0-4}$ elements.

*Collapse simulations*

We were able to validate our architectural model by observing that, when viewed from different orientations, we could simulate the collapse orientations of the component clusters. The first cluster (pm028-18-wy1-C1) contains 15 elements that are highly compressed (Fig. 2A–C), it can be replicated by viewing the model from an oblique rostro-lateral (dextral) orientation, slightly oblique to the horizontal plane (Fig. 2D). This orientation effectively simulates the overlap between the P1, P2 and ramiform array, the 'parallel' arrangement of these elements, and the orthogonal relative arrangement of the P elements versus the 'anterior' (caudal) process of the M elements. Detailed differences between the model and this fused cluster, including the apparently shallower inclination of the $S_{3-4}$ versus the P elements, and the greater apparent separation between the $S_2$ versus $S_{3-4}$ elements, can be rationalized by rotation and the apparent foreshortening of element spacing that results from collapse of the three-dimensional arrangements of the elements in the model to the two-dimensional plane represented by the cluster.

The second cluster (pm028-25-wy1-C1) is composed of 13 elements, including all those anticipated except a pair of $P_1$ elements; the cusps of the M elements are also missing (Fig. 3A–C). This 'oblique' arrangement can be simulated by viewing the model from only a very slightly oblique lateral (dextral) perspective (Fig. 3D), including only a very minor rostral component. In this orientation, we can accurately simulate the very slight rostrad position

of the dextral S and M elements with respect to their sinistral counterparts. Because the collapse orientation is almost purely lateral, the P elements do not collapse to a position in which they overlap and, therefore, fuse together with the S and M elements, hence, the $P_2$ elements are retained in the cluster by a large mass of diagenetic mineral, rather than through overlap with the S and M elements, and the $P_1$ elements are not retained at all. The model accurately reproduces the caudal separation of the $S_2$ from the $S_{3-4}$ elements; this was not achieved in the first cluster and the differences in the efficacy of the model simulation reflect the degree to which the collapse orientation departs from pure lateral. We observed no significant differences between the arrangement of the elements in the model and the cluster except for the orientation of the $P_2$ elements which are parallel to the plane of collapse in the cluster, but approximately perpendicular to this plane in the model. This difference can be rationalized readily in term of gravitationally induced rotation during collapse.

The third cluster (pm028-25-wy1-C2; Fig. 4A–C) preserves a parallel arrangement of the S elements, but with the cusps of the symmetrically-opposing elements displaced dextrally relative to one another. This arrangement can be simulated by viewing the model from the dextral side at about 45° to horizontal plane, with a minor caudal component; this orientation effectively simulates the arrangement of the dextral S and M elements appearing ventral of their sinistral counterparts (Fig. 4D). In detail, the M elements are directed in opposition in the cluster (Fig. 4B–C), rather than in the parallel arrangement simulated in lateral collapse orientations (Figs 2D, 3D). Our model simulation is not exact; the dextral M is oriented approximately perpendicular to the plane of collapse (Fig. 4D) and could settle gravitationally in either a parallel or the opposed orientation seen in the cluster (Fig. 4B–C). In this orientation, the P elements are isolated from the S–M array, precluding their overlap and fusion with the S and M elements during diagenesis; thus, the $P_1$ and $P_2$ elements are not retained within the cluster of S and M elements.

Finally, the fourth cluster (pm028-26-wy1-C1; Fig. 5A–C) includes only S and M elements; the S elements are approximately parallel while the sinistral M element is approximately perpendicular to the alignment of the $S_{1-4}$ elements, and the chord of the dextral M element is parallel to the $S_{1-4}$ elements. The elements are not adpressed and, together with the preserved symmetry in their arrangement, it appears that this cluster has undergone limited post-mortem collapse or compression (Fig. 5B–C). The arrangement of S elements closely approximates the second cluster (Fig. 3A–C) and, similarly, it can be simulated by viewing the model from the side, but with very slightly oblique dorsal and rostral

components (Fig. 5D). In this orientation, the $P_2$ elements overlap partially with the abaxial face of the dextral $S_2$ element (Fig. 5D), but the $P_2$ elements do not occur within the cluster because the elements have not undergone the collapse that would be required for the $P_2$ elements and the dextral $S_2$ element to make contact. The model cannot simulate the arrangement of the M elements which do not retain a bilateral arrangement common to that of the $S_{0-4}$ array of elements; the M elements appear to retain a bilateral arrangement one-to-another, but as a paired unit, they appear to have been rotated laterally through about 90° relative to the $S_{0-4}$ elements. We interpret this deviation from our model as a taphonomic artefact in which the M complex has undergone postmortem reorientation independently of the S array. An alternative interpretation, that this reflects an alternative functional position for the M elements (cf. Goudemand *et al.* 2011) is untenable given that the M and other elements cannot be resolved to a coherent bilateral arrangement in any linear collapse orientation.

## DISCUSSION

### Comparison with other Gondolelloidea

The only member of Gondolelloidea that has been the subject of an architectural apparatus reconstruction is *Novispathodus* (Goudemand *et al.* 2011), based on partial clusters of the S array, and borrowing insight into the relative size and position of the remaining elements from a bedding plane assemblage of *Neogondolella* (Rieber 1980; Orchard & Rieber 1999). The morphology of the element positional homologues in *Novispathodus* and *Nicoraella* are closely comparable, suggesting close phylogenetic affinity. However, the apparatus architectures show significant differences. In particular, the S array of *Novispathodus* has been reconstructed to have a more caudally positioned $S_0$, the rostral processes of the S elements are more widely spaced than in *Nicoraella*, and their caudal processes are more tightly clustered about the plane of bilateral symmetry. The M elements are inferred to have occupied a much more dorsal and rostral position in *Novispathodus*, with their cusps converging in line with those of the $S_{1-2}$ elements. The $P_1$ and $P_2$ elements have been located in close approximation, fully caudad of the S elements in *Novispathodus*, while in *Nicoraella* the $P_2$ and S elements overlap in position on the rostral–caudal axis, and the $P_1$ elements occupy a distinct caudal position.

These differences might reflect taxonomic and phylogenetic differences. Certainly, since most of the clusters we describe reflect lateral collapse orientations, the alignment of the ramiform elements may not be accurately reconstructed in *Nicoraella*. Nevertheless, where critical

differences occur between the inferred apparatus architectures of *Novispathodus* and *Nicoraella*, direct architectural evidence is lacking for *Novispathodus*. Indeed, many aspects of the apparatus architecture of *Novispathodus* were borrowed from *Neogondolella*, or inferred based on ad hoc optimality criteria, like the relative shape of the component elements within the apparatus and what this may imply about their relative positions and functions, as part of a more general 'biomechanical analysis' (Goudemand *et al.* 2011). Unfortunately, there is no intrinsic evidence from *Novispathodus* that discriminates its apparatus architecture from our reconstruction of *Nicoraella*. Indeed, we can simulate the only architectural information for *Novispathodus* on an essentially lateral collapse of the apparatus architecture of *Nicoraella*; the natural assemblage of *Neogondolella* (Fig. 6) (Rieber 1980; Orchard & Rieber 1999; Goudemand *et al.* 2011) can also be rationalized by viewing the *Nicoraella* model from a combined right-lateral, dorsal and slightly caudal perspective (Fig. 6). Thus, we take the apparatus architecture of *Nicoraella* as a more accurate model for *Novispathodus* and *Neogondolella* and, therefore, for Gondolelloidea more generally.

### Comparison with other conodonts

Architectural models exist principally for *Idiognathodus* (Aldridge *et al.* 1987; Purnell & Donoghue 1997, 1998), *Promissum* (Aldridge *et al.* 1995), *Notiodella* (Aldridge *et al.* 2013) and *Panderodus* (Sansom *et al.* 1994). The apparatus architecture of *Nicoraella* exhibits greatest similarity to *Idiognathodus*, which has been shown to also explain natural assemblages of other polygnathaceans (Purnell & Donoghue 1998) *sensu* Donoghue *et al.* (2008), which are members of Ozarkodinina along with the Gondolelloideans (Donoghue *et al.* 2008). When compared with *Idiognathodus*, the apparatus architecture of *Nicoraella* is more compact, with the $P_2$ elements juxtaposed to the S array and the $P_1$ elements occupying a similar relative position to the $P_2$ elements in *Idiognathodus*. In this sense, the apparatus architecture of *Nicoraella* is more akin to that of *Ozarkodina remscheidensis remscheidensis* (Nicoll & Rexroad 1987) which, like *Nicoraella* has distinctly digyrate $S_{1-2}$ elements, as opposed the pseudo-bipennate but strictly extensiform digyrate $S_{1-2}$ elements of *Idiognathodus* (Purnell & Donoghue 1997).

### Implications of apparatus architecture for functional hypotheses

While the history of research into conodont element functional morphology was intimately linked to debate over the biological affinity of conodonts, this changed
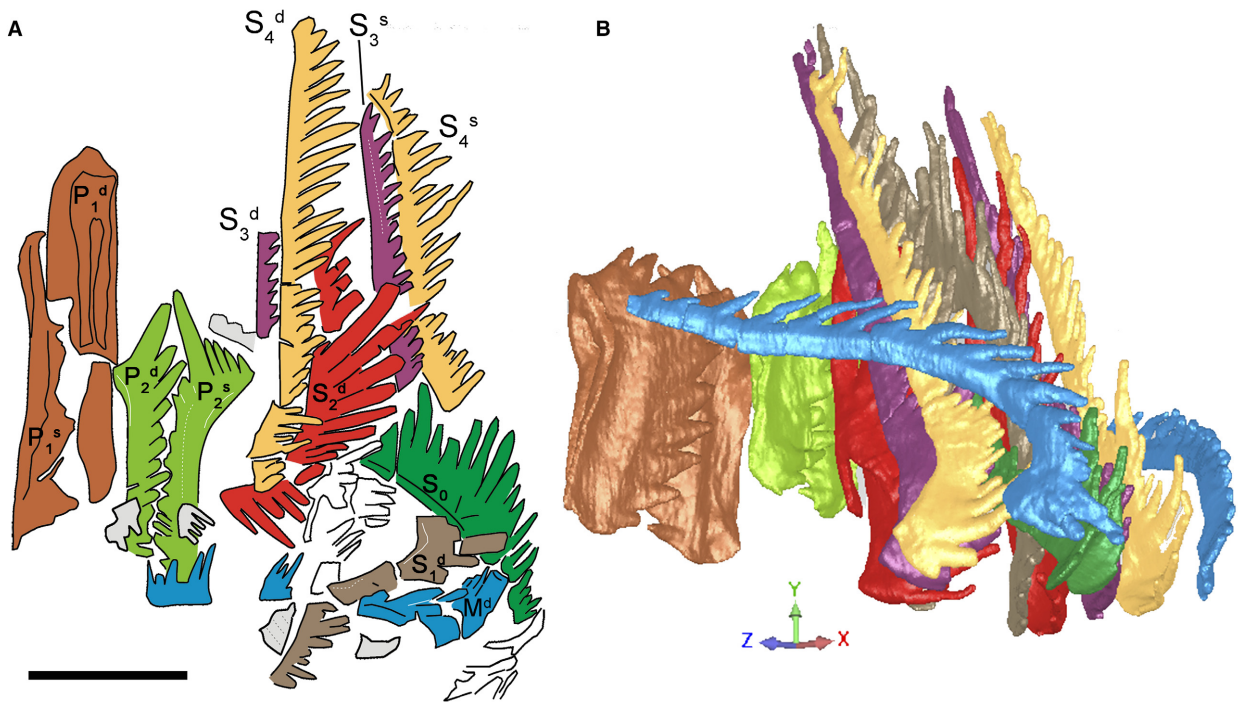
**FIG. 6.** Comparison between a natural assemblage of *Neogondolella* and the reconstructed apparatus of *Nicoraella*. A, camera lucida sketch of a natural assemblage of *Neogondolella* from the Middle Triassic of Monte San Giorgio, Switzerland (based Goudemande *et al.* 2011, fig. 2B). B, the simulated collapse orientation based on our apparatus reconstruction of *Nicoraella kockeli*, viewed from an oblique rostro-lateral orientation with a slight ventral component. Scale bar in A represents 400 μm.

with the discovery of soft tissue remains. Subsequent functional research was constrained by knowledge of apparatus architecture (Aldridge *et al.* 1987; Purnell & Donoghue 1997).

More recently, Goudemand *et al.* (2011) developed a new and more detailed functional interpretation based on *Novispathodus*, basing their inferred arrangement of elements in large part on their biomechanical analysis, apparently deriving independent evidence for the existence of a lingual cartilage, as in the feeding apparatuses of the living cyclostomes. In this model they identify 'growth' and 'cluster' (functional) positions for the elements, based principally upon the complementary morphology exhibited by the elements. A lingual cartilage is imagined to have occupied a space in the arrangement of the elements that could explain movements of the elements inferred from their morphology.

However, as we have shown, the apparatus architecture of *Novispathodus* exhibits incompatibilities with that inferred for the close relative *Nicoraella*, and the primary architectural evidence for *Novispathodus* and *Neogondolella* is better explained by the apparatus architecture inferred for *Nicoraella* (e.g. the collapse orientation for Cluster 1 in Fig. 2). There is no evidence for the 'growth' arrangement of elements for the hypothetical

*Novispathodus* apparatus (Goudemand *et al.* 2011), and the apparatus architecture of *Nicoraella* is incompatible with many of the element motions proposed for *Novispathodus*. For example, the proposed location of a lingual cartilage is precluded by the arrangement of the S elements and, furthermore, much of the rotational motion inferred for the $S_0$ element is precluded by the ventrally and adaxially directed lateral processes of the $S_2$ element, as well as by the $P_2$ elements which are located close to the S array in the apparatus of *Nicoraella*. The proposed motion of the $S_3$ and $S_4$ elements, independently of the $S_2$ and $S_1$ elements, appears unlikely since, in our apparatus model, the $S_2$ elements are aligned with the $S_3$ and $S_4$ elements and, as Goudemand *et al.* (2011) argued, the $S_1$ elements are aligned and encapsulated by the $S_2$ elements.

Of course, it would be possible to develop and refine the biomechanical model of *Novispathodus* (Goudemand *et al.* 2011), accommodating the physical space constraints imposed by the architecture of the apparatus. However, this exercise has perhaps demonstrated that attempts to infer the kinematics of the conodont feeding apparatus based primarily on the complementary morphology of the elements, and based on optimization-based functional interpretation, is not an effective approach (Purnell & Donoghue 1999).

While the functional morphology of Ozarkodinina P elements is comparatively well understood (Donoghue & Purnell 1999; Martínez-Pérez *et al.* 2014*a*, *b*, 2016), the functional interpretation of S and M elements remains the subject of speculation. These ramiforms have been conjectured to perform a role in grasping, but no material evidence has been presented in support of this interpretation, beyond analysis of element growth (Purnell 1994) and analogy based on morphological similarity (Goudemand *et al.* 2011). Rather than guiding anatomical reconstructions, functional interpretations should be constrained by independently derived anatomical reconstructions, such as that presented here for *Nicoraella*, and they could be tested by analysis of recurrent patterns of damage and repair (Purnell & Jones 2012), or through computational and functional experiments of the loads implied by such functional interpretations.

## CONCLUSIONS

The tomographic characterization of exceptional three-dimensionally preserved conodont clusters from early Middle Triassic of Luoping (south-west China) has provided the best evidence for the apparatus architecture and the relative positions of the elements of any gondolelloid, and among the best for any conodont species. The simulation of the different collapse patterns, based on the fused clusters and reproduced through our three-dimensional digital apparatus model, demonstrate the accuracy of our reconstruction. Our study demonstrates that the clusters possessed more of the original skeletal architecture that clearly reflects the relative position of each component element in the apparatus, showing distinct differences with previous proposals. These differences bring a new perspective to understanding conodont skeletal anatomy, functional morphology, and feeding kinematics. In this context, our results allow us to test the architectural and functional models of *Novispathodus* proposed previously by Goudemand *et al.* (2011), demonstrating that their model is contradicted by primary anatomical evidence in the fossils from which it was derived. As such, their apparatus reconstruction and their functional model must be rejected. More importantly, our study exposes the limitations of attempts to reconstruct the anatomical architecture of the conodont apparatus based on functional principles, underlining the importance of discriminating comparative anatomy and functional interpretation in inferring functional morphology in extinct organisms.

## DATA ARCHIVING STATEMENT

Tomographic data and virtual models used in this study are available in the Bristol Digital Repository: https://doi.org/10.5523/bris.p515kyhwv3ec29zo7an2psqju and https://doi.org/10.5523/bris.yw0swm1vgiz92catj97qv8g1c

*Editor.* Andrew Smith

## REFERENCES

ALDRIDGE, R. J. 1987. Conodont palaeobiology: a historical review. 11–34. *In* ALDRIDGE, R. J. (ed.) *Palaeobiology of conodonts*. Ellis Horwood, Chichester.

—— SMITH, M. P., NORBY, R. D. and BRIGGS, D. E. G. 1987. The architecture and function of Carboniferous polygnathacean conodont apparatuses. 63–76. *In* ALDRIDGE, R. J. (ed.) *Palaeobiology of conodonts*. Ellis Horwood, Chichester.

—— BRIGGS, D. E. G., SMITH, M. P., CLARKSON, E. N. K. and CLARK, N. D. L. 1993. The anatomy of conodonts. *Philosophical Transactions of the Royal Society B*, **340**, 405–421.

—— PURNELL, M. A., GABBOTT, S. E. and THERON, J. N. 1995. The apparatus architecture and function of *Promissum pulchrum* Kovács-Endrödy (Conodonta, Upper Ordovician), and the prioniodontid plan. *Philosophical Transactions of the Royal Society B*, **347**, 275–291.

—— MURDOCK, D. J. E., GABBOTT, S. E. and THERON, J. N. 2013. A 17-element conodont apparatus from the Soom Shale Lagerstätte (Upper Ordovician), South Africa. *Palaeontology*, **56**, 261–276.

BRIGGS, D. E. G. and FORTEY, R. A. 1982. The cuticle of the aglaspidid arthropods, a red-herring in the early history of the vertebrates. *Lethaia*, **15**, 25–29.

—— and WILLIAMS, S. H. 1981. The restoration of flattened fossils. *Lethaia*, **16**, 1–14.

COLLINSON, C., AVCIN, M. C., NORBY, R. D. and MERRILL, G. K. 1972. Pennsylvanian conodont assemblages

from La Salle County, northern Illinois. *Illinois State Geological Survey Guidebook Series*, **10**, 1–37.

DONOGHUE, P. C. J. and PURNELL, M. A. 1999. Mammal-like occlusion in conodonts. *Paleobiology*, **25**, 58–74.

—— BENGTSON, S., DONG, X.-P., GOSTLING, N. J., HULDTGREN, T., CUNNINGHAM, J. A., YIN, C., YUE, Z., PENG, F. and STAMPANONI, M. 2006. Synchrotron X-ray tomographic microscopy of fossil embryos. *Nature*, **442**, 680–683.

—— PURNELL, M. A., ALDRIDGE, R. J. and ZHANG, S. 2008. The interrelationships of 'complex' conodonts (Vertebrata). *Journal of Systematic Palaeontology*, **6**, 119–153.

GOUDEMAND, N., ORCHARD, M. J., URDY, S., BUCHER, H. and TAFFOREAU, P. 2011. Synchrotron-aided reconstruction of the conodont feeding apparatus and implications for the mouth of the first vertebrates. *Proceedings of the National Academy of Sciences*, **108**, 8720–8724.

HU, S. X., ZHANG, Q. Y., CHEN, Z. Q., ZHOU, C. Y., LU, T., XIE, T., WEN, W., HUANG, J. Y. and BENTON, M. J. 2011. The Luoping biota: exceptional preservation, and new evidence on the Triassic recovery from end-Permian mass extinction. *Proceedings of the Royal Society B*, **278**, 2274–2282.

HUANG, J., ZHANG, K., ZHANG, Q., LÜ, T., ZHOU, C. and BAI, J. 2009. Conodonts stratigraphy and sedimentary environment of the Middle Triassic at Daaozi section of Luoping County, Yunnan Province, south China. *Acta Micropalaeontologica Sinica*, **26**, 211–224.

—— —— —— —— HU, S. and ZHOU, C. 2011. Advance research of conodont fauna from Shangshikan and Daaozi sections in Luoping area, Yunnan Province. *Geological Science & Technology Information*, **30**, 1–17.

—— MARTÍNEZ-PÉREZ, C., HU, S.-X., DONOGHUE, P. C. J., ZHANG, Q.-Y., ZHOU, C.-Y., WEN, W., BENTON, M. J., LUO, M., YAO, H.-Z. and ZHANG, K.-X. 2018. Data from: Middle Triassic conodont apparatus architecture revealed by synchrotron X-ray microtomography. Bristol Digital Repository. https://doi.org/10.5523/bris.yw0swm1vgiz92catj97qv8g1c

—— —— —— ZHANG, Q., ZHANG, K., ZHOU, C., WEN, W., XIE, T., BENTON, M. J., CHEN, Z.-Q., LUO, M. and DONOGHUE, P. C. J. 2019a. Data from: Apparatus architecture of the conodont *Nicoraella kockeli* (Gondolelloidea, Prioniodinina) constrains functional interpretations. *Bristol Digital Repository*. https://doi.org/10.5523/bris.p515kyhwv3ec29zo7an2psqju

—— HU, S., ZHANG, Q., DONOGHUE, P. C. J., BENTON, M. J., ZHOU, C., MARTÍNEZ-PÉREZ, C., WEN, W., XIE, T., CHEN, Z.-Q., LUO, M., YAO, H. and ZHANG, K. 2019b. Gondolelloid multielement conodont apparatus (*Nicoraella*) from the Middle Triassic of Yunnan Province, southwestern China. *Palaeogeography, Palaeoclimatology, Palaeoecology*, **522**, 98–110.

—— MARTÍNEZ-PÉREZ, C., HU, S.-X., DONOGHUE, P. C. J., ZHANG, Q.-Y., ZHOU, C.-Y., WEN, W., BENTON, M. J., LUO, M., YAO, H.-Z. and ZHANG, K.-X. in press. Middle Triassic conodont apparatus architecture revealed by synchrotron X-ray microtomography. *Palaeoworld*,

available online 23 August 2018. https://doi.org/10.1016/j.palwor.2018.08.003

MARONE, F., MÜNCH, B. and STAMPANONI, M. 2010. Fast reconstruction algorithm dealing with tomography artifacts. *Developments in X-Ray tomography VII*, Proceedings SPIE, **7804**, 780410.

MARTÍNEZ-PÉREZ, C., PLASENCIA, P., JONES, D., KOLAR-JURKOVŠEK, T., SHA, J., BOTELLA, H. and DONOGHUE, P. C. J. 2014a. There is no general model for occlusal kinematics in conodonts. *Lethaia*, **47**, 547–555.

—— RAYFIELD, E. J., PURNELL, M. A. and DONOGHUE, P. C. J. 2014b. Finite element, occlusal, microwear and microstructural analyses indicate that conodont microstructure is adapted to dental function. *Palaeontology*, **57**, 1059–1066.

—— —— BOTELLA, H. and DONOGHUE, P. C. J. 2016. Translating taxonomy into the evolution of conodont feeding ecology. *Geology*, **44**, 247–250.

MASTANDREA, A., IETTO, F., NERI, C. and RUSSO, F. 1997. Conodont biostratigraphy of the late Triassic sequence of Monte Cocuzzo (Catena Costiera, Calabria, Italy). *Rivista Italiana di Paleontologia e Stratigrafia*, **103**, 173–182.

NICOLL, R. S. 1982. Multielement composition of the conodont *Icriodus expansus* Branson & Mehl from the Upper Devonian of the Canning Basin, Western Australia. *BMR Journal of Australian Geology & Geophysics*, **7**, 197–213.

—— 1985. Multielement composition of the conodont species *Polygnathus xylus xylus* Stauffer, 1940 and *Ozarkodina brevis* (Bischoff and Ziegler, 1957) from the Upper Devonian of the Canning Basin, Western Australia. *Bureau of Mineral Resources Journal of Australian Geology & Geophysics*, **9**, 133–147.

—— and REXROAD, C. B. 1987. Re-examination of Silurian conodont clusters from northern Indiana. 49–61. *In* ALDRIDGE, R. J. (ed.) *Palaeobiology of conodonts*. Ellis Horwood, Chichester.

ORCHARD, M. J. and RIEBER, H. 1999. Multielement *Neogondolella* (Conodonta, upper Permian – middle Triassic). *Bollettino Della Società Paleontologica Italiana*, **37**, 475–488.

PURNELL, M. A. 1994. Skeletal ontogeny and feeding mechanisms in conodonts. *Lethaia*, **27**, 129–138.

—— and DONOGHUE, P. C. J. 1997. Skeletal architecture and functional morphology of ozarkodinid conodonts. *Philosophical Transactions of the Royal Society B*, **352**, 1545–1564.

—— —— 1998. Skeletal architecture, homologies and taphonomy of ozarkodinid conodonts. *Palaeontology*, **41**, 57–102.

—— —— 1999. Flattened fossils, physical modelling and the restoration of collapsed skeleton. 91–99. *In* SAVAZZI, E. (ed.) *Functional morphology of the invertebrate skeleton*. John Wiley & Sons.

—— and JONES, D. O. 2012. Quantitative analysis of conodont tooth wear and damage as a test of ecological and functional hypotheses. *Paleobiology*, **38**, 605–626.

—— DONOGHUE, P. C. J. and ALDRIDGE, R. J. 2000. Orientation and anatomical notation in conodonts. *Journal of Paleontology*, **74**, 113–122.

RIEBER, H. 1980. Ein conodonten-cluster aus der Grenzbitumenzone (Mittlere Trias) des Monte San Giorgio (Kt. Tessin/

Schweiz). *Annalen des Naturhistorischen Museums Wien*, **83**, 265–274.

SANSOM, I. J., ARMSTRONG, H. A. and SMITH, M. P. 1994. The apparatus architecture of *Panderodus* and its implications for coniform conodont classification. *Palaeontology*, **37**, 781–799.

SCHMIDT, H. 1934. Conodonten-Funde in ursprünglichem zusammenhang. *Paläontologische Zeitschrift*, **16**, 76–85.

SCHÜLKE, I. 1997. Conodont clusters and multielement reconstructions from the Upper Kellwasser horizon at La Serre (Late Frasnian, Montagne Noire, Southern France). *Geologica et Palaeontologica*, **31**, 37–66.

SCOTT, H. W. 1934. The zoological relationships of the conodonts. *Journal of Paleontology*, **8**, 448–455.

ZHANG, Q.-Y., ZHOU, C.-Y., LU, T., XIE, T., LOU, X.-Y., LIU, W., SUN, Y.-Y., HUANG, J.-Y. and ZHAO, L.-S. 2009. A conodont-based Middle Triassic age assignment for the Luoping Biota of Yunnan, China. *Science in China Series D: Earth Sciences*, **52**, 1673–1678.